

Interaction of Low-Energy Electrons with the Purine Bases, Nucleosides, and Nucleotides of DNA

Carl Winstead and Vincent McKoy

A. A. Noyes Laboratory of Chemical Physics

California Institute of Technology

Pasadena, California 91125

(Dated: November 27, 2006)

Abstract

We report results from computational studies of the interaction of low-energy electrons with the purine bases of DNA, adenine and guanine, as well as with the associated nucleosides, deoxyadenosine and deoxyguanosine, and the nucleotide deoxyadenosine monophosphate. Our calculations focus on the characterization of the π^* shape resonances associated with the bases but also provide general information on the scattering of slow electrons by these targets. Results are obtained for adenine and guanine both with and without inclusion of polarization effects, and the resonance energy shifts observed due to polarization are used to predict π^* resonance energies in associated nucleosides and nucleotides, for which static-exchange calculations were carried out. We observe slight shifts between the resonance energies in the isolated bases and those in the nucleosides.

PACS numbers: 34.80.Bm

I. INTRODUCTION

The observation that slow electrons cause damage to DNA, including single- and double-strand breaks [1–5], has stimulated considerable interest in gas- and condensed-phase studies of low-energy electron interactions with the constituents of DNA and RNA [6]. Peaks in the damage rate as a function of electron energy indicate that resonant processes are involved. Accordingly, most studies initially focused on the purine and pyrimidine nucleobases and their halogenated, methylated, or deuterated derivatives, the π^* resonances associated with the aromatic ring systems of the bases being obvious candidates for the formation of temporary anions. Experimental studies of the nucleobases or their derivatives have overwhelmingly focused on dissociative attachment (DA) [7–12, 14, 15, 17–31], though a few have examined electron-impact excitation [32–37] and ionization [19, 31, 38]. This effort has revealed the bond-selective nature of low-energy DA [16, 23–27] and the important role that vibrational Feshbach resonances associated with dipole-bound anion states appear to play in driving such dissociation [15, 23, 27]. No gas-phase total or elastic scattering cross section measurements for the nucleobases have, to our knowledge, been reported, except for the relative 90° differential cross sections for uracil and halouracils obtained by Abouaf and Dunet [21]. However, Aflatooni, Gallup, Burrow and coworkers [15, 39] have conducted valuable studies of the electron transmission spectra for the nucleobases that reveal the energies of resonances in the low-energy total scattering cross section, and they have assigned the features they see to π^* shape resonances. The few calculations that have been made of electron cross sections for nucleobases have mostly relied on one-electron, potential-scattering models [40–43] and have produced low-energy elastic cross sections whose resonance positions disagree with the experimentally-determined positions [15, 39, 41, 43, 44]. We recently reported results from all-electron cross section calculations for uracil [45], including elastic cross sections whose resonance positions are in somewhat better agreement with experiment [15, 39] as well as initial cross sections for electron-impact excitation.

Increasing attention is now being given to the sugar-phosphate backbone of DNA, in large part because of electronic-structure studies by Simons and coworkers [46–49] that suggested electrons initially trapped on one of the bases may be transferred to the backbone and there promote breaking of the phosphodiester C–O bonds linking the sugar and phosphate groups. Li and coworkers [50, 51] and Gu and coworkers [52–59] have carried

out related electronic-structure studies of nucleoside (base + sugar) and nucleotide (nucleoside + phosphate) neutrals, anions, and radicals with a view to elucidating the energetics of electron attachment and of cleaving both the phosphodiester C–O bonds of the backbone and the N-glycosidic base–sugar bonds. Condensed-phase experiments on thymidine and a single-strand oligonucleotide have demonstrated that slow electrons do indeed break the C–O phosphate-sugar bonds as well as the C–N base-sugar bonds [60–62], and C–O bond breaking was also found in gas-phase DA to a model phosphodiester [63]. A few electron-collision studies, experimental and theoretical, have looked at the individual backbone constituents, i.e., ribose or deoxyribose and a phosphate group [64–69], and others have also been made of electron collisions with backbone analogues such as tetrahydrofuran [29, 65, 68–79], tetrahydrofurfuryl alcohol [71, 72, 80, 81], fructose [79], and dibutyl phosphate [63]. However, the only electron collision measurements involving nucleosides that we are aware of are the study by Zheng and coworkers of thymine desorption from condensed-phase deoxythymidine [60], mentioned earlier, and the gas-phase studies by Abdoul-Carime and coworkers [82] and by Denifl and coworkers [83] of DA to, respectively, deoxythymidine and 5-bromouridine. The only electron collision calculation on a larger moiety appears to be our recent study of the 5' phosphate ester of deoxyribose [68].

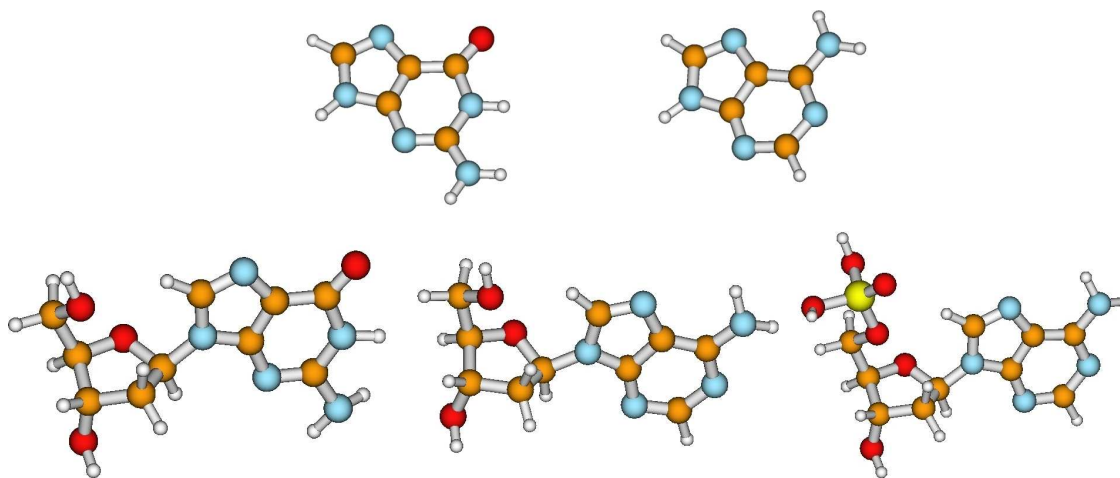


FIG. 1: (Color online) The molecules considered in the present work. On the top row are the purine bases guanine (left) and adenine (right); on the bottom row, left to right, are the nucleosides 2'-deoxyguanosine and 2'-deoxyadenosine and the nucleotide 2'-deoxyadenosine 5'-monophosphate. Oxygen is red (dark), carbon brown (medium), nitrogen blue (light), and hydrogen white; phosphorous is the light-yellow sphere surrounded by four oxygens.

Clearly, much additional work is needed to elucidate the interactions of low-energy electrons both with isolated nucleobases and with larger assemblies that may give insight into proposed strand-breaking mechanisms. In the present paper, we apply the Schwinger multichannel (SMC) method [84, 85] to study elastic electron scattering by the purine bases adenine (A) and guanine (G), with an emphasis on determining the energies of π^* resonances in the scattering cross section. To make a closer connection between our results for these isolated molecules and DNA itself, we also study elastic scattering by the purine nucleosides 2'-deoxyadenosine (dA) and 2'-deoxyguanosine (dG), as well as by the nucleotide 2'-deoxyadenosine 5'-monophosphate (dAMP). (See Fig. 1 for the molecular structures.) Although we cannot carry out calculations on the larger moieties at as high a level as is possible for A and G with present versions of our computer codes, comparison between high- and low-level calculations on A and G yields energy shifts that we apply to predict resonance positions in the larger species.

The next section gives details of the calculations. Sec. III contains the results and discussion, and Sec. IV summarizes our results.

II. COMPUTATIONAL DETAILS

The Schwinger multichannel method [84, 85] and its implementation [86, 87] have been described elsewhere. Here we give only the particulars of the present calculations.

We optimized the ground-state nuclear geometries of A and G at the level of second-order Møller-Plesset perturbation theory (MP2) within the 6-31G(*d*) basis set, using either GAMESS [88] or Gaussian 94 [89]. MP2/6-31G(*d*) geometries for dA and dG were taken from the work of Foloppe and MacKerell [90], in both cases using the geometry optimized for the “south” pseudorotational conformer of the furanose ring, which predominates in B-type DNA [90]. To obtain a geometry for dAMP, we replaced the OH group attached to the 5' carbon in the dA geometry of Ref. [90] with an H₂PO₄ group, using bond distances and angles taken from our previously-computed MP2/6-31G(*d*) geometry for deoxyribose 5'-monophosphate [68] to fix the positions of the added atoms. The resulting structures are shown in Fig. 1, which was generated using MOLDEN [91].

Both A and G are nearly planar molecules, with the largest departure from plane geometry involving the hydrogens of the amine group. Imposing a planar geometry on each molecule

facilitates both the computations and their analysis by allowing us to separate the orbitals and overall electronic states into representations of the C_s point group; in particular, the π^* shape resonances fall into the ${}^2A''$ representation and are more readily distinguishable from the large ${}^2A'$ background. However, distorting the molecular geometry may shift resonance positions, as we recently found, for example, in tetrahydrofuran [68]. Accordingly, while we carried out most of our A and G calculations for geometries constrained to be planar, we also carried out SE calculations on G at an undistorted, C_1 geometry to determine the effect of imposing plane symmetry. Comparison of the C_s and C_1 results indicates that the π^* resonances are shifted upward in energy by about 0.2 eV in the C_s conformation.

We used several one-electron basis sets in the present work. For the SEP calculations on A and G, we used the 6-311++G(d,p) basis set as defined within GAMESS [88], which we will call Basis I hereafter. For most of the SE calculations, we used a Basis II consisting of the “double-zeta” basis set of Dunning and Hay [92] together with, on the heavy atoms, a $1s1p$ diffuse supplement and two d polarization functions and, on the hydrogens, a $1s$ diffuse supplement and one p polarization function; the GAMESS default values were used for all exponents and splitting factors in this supplement. Some of the SE calculations were carried out in a Basis III that comprised Dunning’s “triple-zeta” basis set [93] together with a $1s1p$ diffuse and $3d$ polarization supplement on the heavy atoms and a $1s$ diffuse and $2p$ polarization supplement on the hydrogens, again using GAMESS’s default exponents and splitting factors. Finally, as a convergence check we also carried out SE calculations on A in a very large basis, Basis IV, formed by supplementing the TZV basis with an array of s Gaussians on a grid of centers and a set of diffuse functions at the positive end of the molecule. For this basis we used the same s grid and diffuse supplement as in previous work on uracil [45], with appropriate shifts in position to roughly center the grid on A’s center of mass and to place the extra diffuse functions beyond the end of the molecule. As will be shown below, the only significant changes from basis set to basis set are in the background scattering cross section at very low energy and in the overall cross section magnitude above the highest π^* resonance energy. Accordingly, most of the SE calculations for dG, dA, and dAMP were carried out in Basis II.

For the ${}^2A''$ symmetry of A and G, we included polarization effects by adding closed-channel terms to the $(N + 1)$ -particle variational space. To form these closed-channel terms, we first transformed the virtual orbitals into modified virtual orbitals (MVOs) using a +6

ionic Fock operator [94]. The three lowest-energy a'' MVOs were then coupled with all singlet-coupled, singly-excited N -electron configurations that could be formed by exciting from an occupied valence orbitals into an empty orbital of the same symmetry. This procedure is intended to describe well the relaxation of the target molecule’s charge density in the presence of an electron temporarily trapped in a π^* orbital, within a variational space of manageable size. It results in a ${}^2A''$ variational space of 10280 ${}^2A''$ configuration state functions (CSFs) for A and 12349 CSFs for G.

The adequacy of the numerical quadrature used to evaluate the interaction-free Green’s function was tested both on- and off-shell. For the off-shell quadrature, we found it sufficient to use a Lebedev [95] angular quadrature scheme of order 41 up to $|\vec{k}| = 2$ atomic units, order 59 from $|\vec{k}| = 2$ to 4, and order 89 above $|\vec{k}| = 4$. In SE calculations on A and dA, this quadrature scheme gave essentially the same results as were obtained using a substantially larger angular quadrature (order 59 below $|\vec{k}| = 2$, order 89 from 2 to 4, and order 101 above 4). The on-shell angular quadratures varied from order 23 to 41, depending on the impact energy and the size of the target molecule, and were chosen so that the orientationally-averaged integral and forward- and backward-scattering cross sections computed directly from the quadrature agreed to within $\sim 1\%$ or better with those obtained after expanding the exit-channel scattering amplitude in partial waves. Partial-wave expansions were carried out at least up to $\ell = 14$ and, if necessary to obtain convergence, as high as $\ell = 22$. The radial quadrature in the off-shell Green’s function employed 108 points, 64 Gauss–Legendre points below $|\vec{k}|=4$ and 44 Gauss–Laguerre points above.

All of the molecules considered here possess dipole moments, some of them quite large, and long-range scattering of electrons by the dipole potential leads to a very large forward scattering cross section that generally will not be captured by computational methods that rely on finite basis sets and/or partial-wave expansions. Procedures exist for correcting calculated results to account for such long-range scattering [96]; however, in the present work we have neglected such corrections because they are not expected to significantly affect the π^* resonance energies.

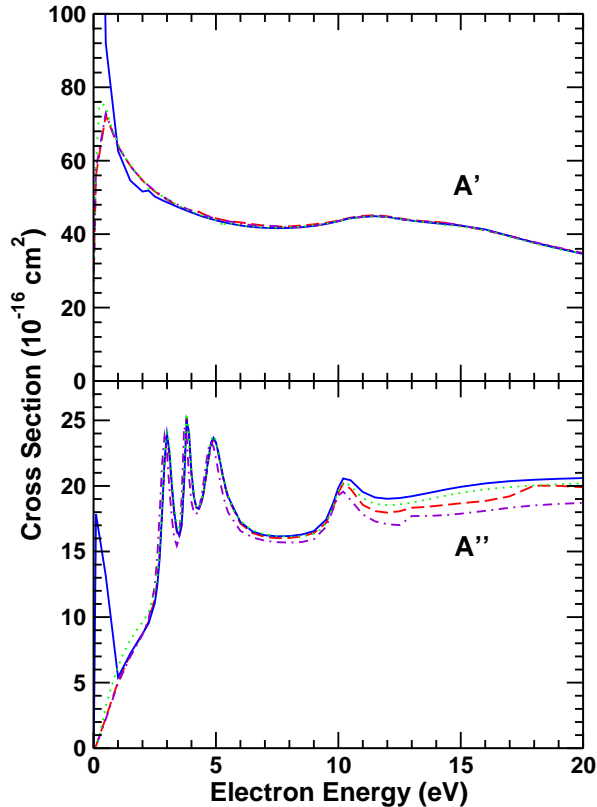


FIG. 2: (Color online) Integral elastic cross sections for adenine computed in the static-exchange approximation using different basis sets: Basis I (chained, violet), Basis II (red, dashed), Basis III (green, dotted), and Basis IV (blue, solid). The top panel shows results for the A' component of the C_s point group and the bottom panel for the A'' component, where the π^* resonances occur.

III. RESULTS AND DISCUSSION

A. Adenine

In Fig. 2, we compare integral cross sections for elastic scattering of electrons by adenine computed in the SE approximation using basis sets I, II, III, and IV. The contributions from wavefunctions transforming according to the A' and A'' components of the C_s point group are shown separately; the latter component contains the π^* shape resonances, which appear as 3 narrow peaks in the 3–5 eV energy range and a fourth peak just above 10 eV. Broad A' features, probably due to overlapping σ^* resonances, are visible at about 11 and 15 eV. The main point to note is that the cross sections, including the peak locations, are insensitive to the choice of basis set; Basis I places the π^* resonances about 0.1 to 0.2 eV

lower than the other three bases, which are in close agreement with each other. The most significant changes in the cross sections are at energies above 10 eV, where the larger basis sets give somewhat larger cross sections, and at energies below about 2 eV, where basis IV, the largest and spatially the most extensive, begins to capture the enhancement of the cross section by long-range interactions between the electron and the permanent electric dipole moment of A.

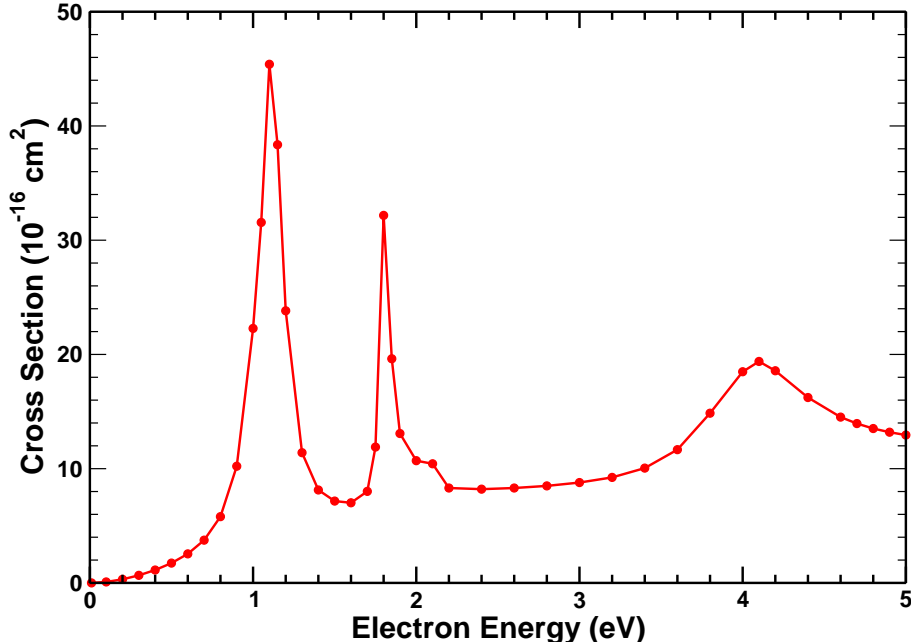


FIG. 3: (Color online) A'' component of the low-energy integral cross section for elastic scattering of electrons by adenine computed in the SEP approximation.

The results for the A'' component obtained in the SEP approximation using Basis I are shown in Fig. 3. We only show results up to 5 eV because results at higher energy are significantly affected by pseudoresonances, making it difficult to determine the actual location of the fourth π^* resonance. With polarization included, the first three resonances shift downward to about 1.1, 1.8, and 4.1 eV. Comparing our SEP energies to the experimental resonance positions, 0.54, 1.36, and 2.17 eV, [39], we see that our calculated positions are too high by about half an eV for the lowest two resonances and about 2 eV for the third. The pattern here is similar to that which we saw for the pyrimidine base uracil [45], with a larger energy mismatch for the higher-energy resonances. As shown immediately below for

G, perhaps 0.2 eV of the discrepancy with experiment arises because we have constrained A to a planar geometry. The remaining discrepancy may in part arise from limitations in our treatment of polarization. In particular, the larger discrepancy for the third resonance may reflect the restriction to configurations chosen to describe core relaxation in a shape resonance. If, for example, the higher π^* resonances mix strongly with core-excited resonances built on low-lying $\pi \rightarrow \pi^*$ or $n \rightarrow \pi^*$ triplet states, the energy shifts due to such mixing would not be fully captured in our present configuration space. We intend to explore this issue in future work.

The calculations of Tonzani and Greene [43] yield 2.4, 3.2, 4.4 and 9 eV for the π^* resonance energies in A, somewhat higher than the energies we obtain, especially for the first two resonances. These authors employ a one-electron scattering model in which local potentials approximate the exchange and polarization interactions. Both approximations may introduce errors, but because the SE energy for the ${}^2\Pi_u$ shape resonance of CO₂ computed by the same method is about 2 eV higher than that obtained in accurate, all-electron SE calculations [97], it seems likely that the approximation to exchange is the main source of error in their results for A.

B. Guanine

Integral elastic cross sections for G computed in the static-exchange approximation within Basis III are shown in Fig. 4. As we did for A, we show the symmetry components obtained from a calculation where the nuclei were constrained to C_s symmetry. Despite small changes in resonance energies, there is strong similarity to the A results of Fig. 2, with the main qualitative difference being that the two lowest-energy π^* resonances in G are so closely spaced as to merge into a single asymmetric peak. To gauge the effect of constraining the nuclear geometry to C_s , the bottom panel of the Fig. 4 compares the C_s integral cross section with that calculated at a fully optimized, C_1 nuclear geometry. Relaxing the geometry constraint shifts the π^* resonance energies lower by about 0.2 eV. We can expect comparable shifts to apply to the SEP results for G and to the SE and SEP results for A.

The effect of polarization on the π^* resonance positions is shown in Fig. 5, where we present our SEP results for the A'' component of the low-energy G elastic cross section obtained in C_s symmetry with Basis I. This calculation places the three lowest π^* resonances

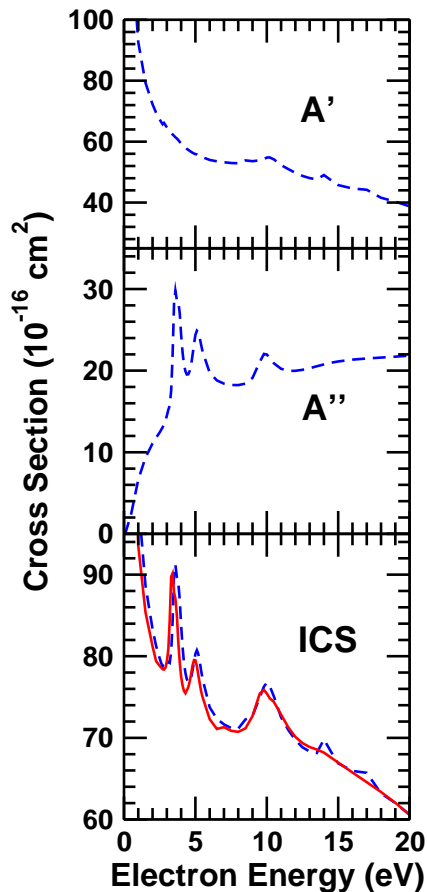


FIG. 4: (Color online) Integral elastic cross sections for guanine computed in the static-exchange approximation using basis set Basis III. Components of the cross section obtained in C_s symmetry are shown in the top two panels. The bottom panel compares the summed C_s cross section (dotted blue line) with the integral cross section obtained using the fully-optimized C_1 nuclear geometry (solid red line).

at about 1.55, 2.4, and 3.75 eV, versus experimental resonance positions [39] of 0.46, 1.37, and 2.36 eV; the calculation of Tonzani and Greene [43] gives 2.4, 3.8, and 4.8 eV. Clearly, there is a much bigger discrepancy between the SEP and experimental positions for the first two π^* resonances for G than we saw above for A. The likely explanation is that the electron-transmission measurements and calculations are looking at different G tautomers. Afatooni, Scheer, and Burrow already noted [39], in comparing their observed resonance energies to predictions based on shifted virtual-orbital energies, that better agreement results

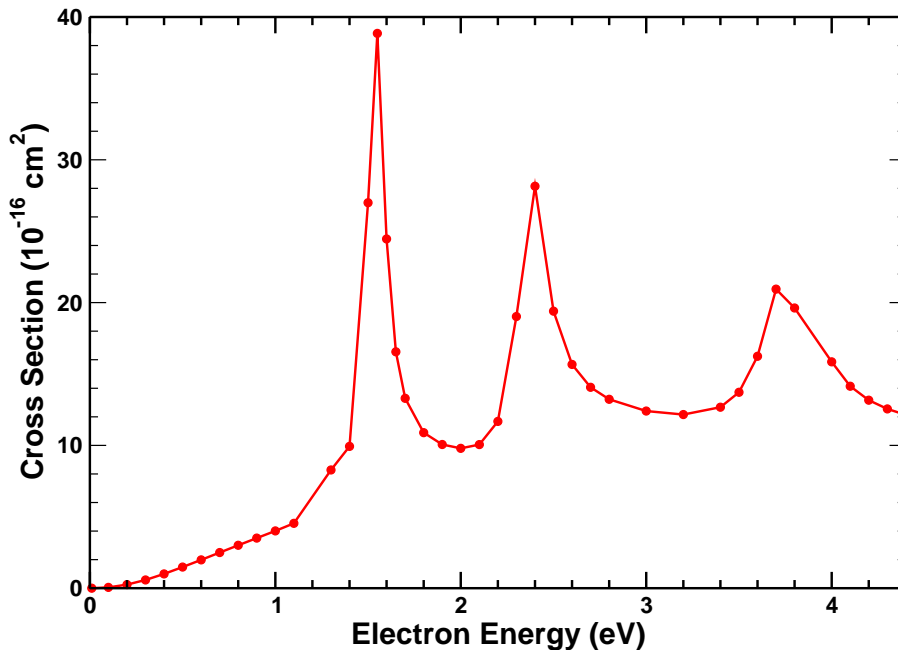


FIG. 5: (Color online) A'' component of the low-energy integral cross section for elastic scattering of electrons by guanine computed in the SEP approximation.

if one assumes gas-phase G is primarily in an enol form rather than the keto form shown in Fig. 1, which is the form found in DNA base pairs. Spectroscopic observations [98] support the conclusion that enol tautomers of G dominate in the gas phase. (In contrast, only one tautomer, identified as the 9H-keto form shown in Fig. 1, is observed in gas-phase A [99].) We can speculate, therefore, that the first two π^* resonances for the 9H-keto tautomer of G should in fact occur at about 1.0 and 1.6 eV, based on our SEP energies for G and the half-volt difference between experiment and theory we saw for A.

C. Larger Moieties

In Fig. 6 we compare the integral elastic cross sections computed for the nucleosides dG and dA and for the nucleotide dAMP. All of these results are obtained in the static-exchange approximation, using basis II for dA and dAMP and basis III for dG. Because of the lack of symmetry in these molecules, we can no longer separate the π^* resonances cleanly from the background, as was possible for A and G, but the resonance positions are nonetheless clearly visible in the full integral cross sections shown in Fig. 6.

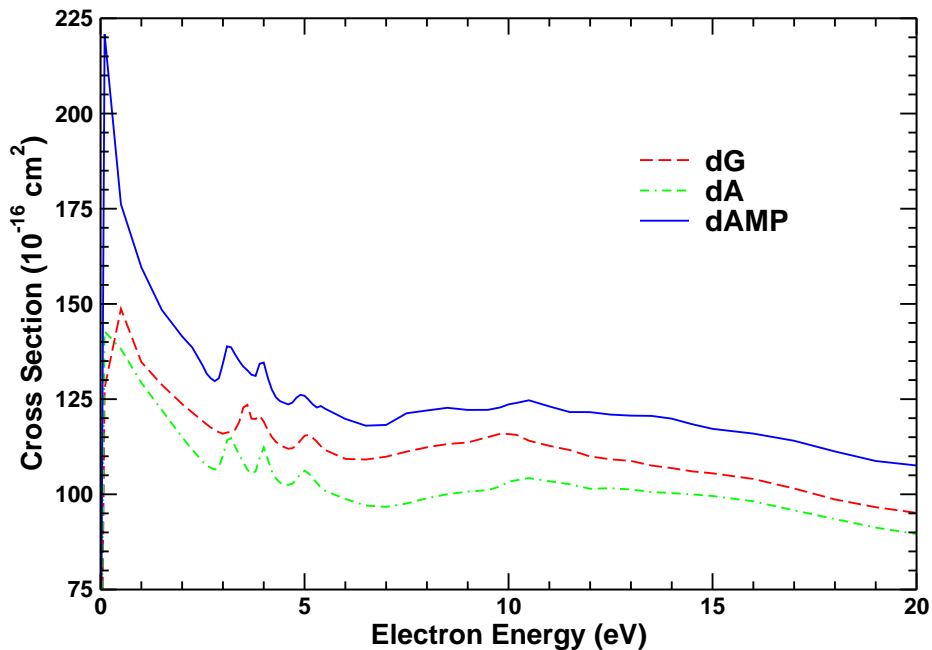


FIG. 6: (Color online) Integral elastic electron scattering cross sections for the nucleosides 2'-deoxyguanosine (dashed red line), 2'-deoxyadenosine (dashed green line), and the nucleotide 2'-deoxyadenosine 5'-monophosphate (solid blue line), computed in the static-exchange approximation.

One interesting result we can immediately note is that there are small but systematic shifts in resonance position between the isolated nucleobases and the corresponding nucleosides. Specifically, Fig. 6 shows that the lowest 3 π^* resonances in dA are found at about 3.2, 4.0, and 5.0 eV, whereas our SE results for A (Fig. 2) place the lowest π^* resonances 0.1 to 0.2 eV lower, at about 3.0, 3.8, and 4.9 eV. As discussed above, our imposition of planar geometry on the amino group of A, an approximation not made in the calculation on dA, may shift the π^* resonances upward, so the actual change in going from A to dA may be slightly larger than 0.1–0.2 eV. A similar pattern is found when comparing G and dG. The 3 lowest π^* resonances in the SE cross section for dG occur at about 3.55, 3.9, and 5.05 eV, as determined by fitting Lorentzians to the two lowest, overlapping peaks. The corresponding SE results for the fully optimized C_1 geometry of G are about 3.35, 3.6, and 4.95 eV, and thus lower by 0.1 to 0.3 eV than in dG. Assuming these shifts carry over after polarization effects are included, we therefore predict that *the lowest 3 π^* resonances are destabilized by*

about 0.1–0.3 eV in the purine nucleosides compared to the corresponding isolated bases.

On the other hand, there is virtually no change in the π^* resonance positions in going from dA to dAMP. The largest shift occurs for the third peak, and it is less than 0.1 eV. For this reason, we did not carry out calculations on deoxyguanosine monophosphate. Of course, this apparent convergence does not at all rule out other environmental effects on the π^* resonance positions in DNA, such as those that might arise from base pairing, base stacking, or solvation, and we intend to explore such effects in future calculations.

Another feature worth noting in Fig. 6 is the broad enhancement of all three cross sections in the 7–9 eV energy range, visible as a shoulder in dG and dA and as a weak maximum in dAMP. This feature is not present in the SE cross sections for A and G (Figs. 2 and 4), which exhibit broad A' maxima (presumably due to σ^* resonances) at about 10 eV that appear to give rise to separate features at or above 10 eV in the dG, dA, and dAMP cross sections of Fig. 6. In a recent study of tetrahydrofuran, deoxyribose, and deoxyribose 5'-monophosphate [68], we found a broad peak at 10 eV in the SE cross section for tetrahydrofuran that appeared to broaden toward lower energy in deoxyribose and its phosphate ester, but again no separate feature between 7 and 9 eV. The only type of bond found in the nucleosides and nucleotides that is not found in the other molecules mentioned is the N-glycosidic base-sugar bond, so it is natural to speculate that the feature at 7–9 eV is associated with a C–N σ^* resonance antibonding between base and sugar. If that speculation were correct, then applying a typical polarization shift of 2 eV to our SE results would imply that the actual C–N σ^* resonance should be found in the 5–7 eV range. In this regard, it is interesting that Zheng and coworkers [62] observe a peak or shoulder at 6 eV in G release from thin molecular films of DNA oligomer bombarded by energy-selected electrons. On the other hand, no such feature is visible in the A release profile, although a clear maximum is seen at 10 eV for both A and G. Moreover, test calculations on dA in which we selectively deleted configurations from the variational space did not show an association between the 7–9 eV enhancement and C–N antibonding configurations. The origin of this feature thus remains unclear but probably does not lie in a base–sugar σ^* resonance.

IV. SUMMARY

We have reported cross sections for elastic electron scattering by adenine, guanine, 2'-deoxyadenosine, 2'-deoxyguanosine, and 2'-deoxyadenosine 5'-monophosphate. Our best (SEP) values for the energies of the π^* shape resonances in G and A are closer to the experimental resonance positions than earlier calculated results. The remaining discrepancy between our results and the measurements can be attributed in part to limitations in our treatment of polarization and to our imposition of C_s symmetry. Comparison of the SE cross sections for dG and dA with those for G and A indicates that the 3 lowest π^* resonances are shifted upward by 0.1–0.3 eV in the nucleosides vs. the nucleobases, but that the energy shifts between A and dA are negligible.

In future work, we hope to clarify the role of shape resonances in DNA strand breaks by examining the effects of base pairing or stacking on resonance positions. We also intend to examine the possible role of shape resonances centered on the backbone, which have been proposed as an initial attachment mechanism leading to phosphodiester bond cleavage [50, 63, 66].

Acknowledgments

We gratefully acknowledge support of this work by the U.S. Department of Energy, Office of Basic Energy Sciences, and use of the computational resources of the Caltech–JPL Supercomputing Project.

-
- [1] B. Boudaïffa, P. Cloutier, D. Hunting, M. A. Huels, and L. Sanche, *Science* **287**, 1658 (2000).
 - [2] B. Boudaïffa, P. Cloutier, D. Hunting, M. A. Huels, and L. Sanche, *Radiat. Res.* **157**, 227 (2002).
 - [3] M. A. Huels, B. Boudaïffa, P. Cloutier, D. Hunting, and L. Sanche, *J. Am. Chem. Soc.* **125**, 4467 (2003).
 - [4] F. Martin, P. D. Burrow, Z. Cai, P. Cloutier, D. Hunting, and L. Sanche, *Phys. Rev. Lett.* **93**, 068101 (2004).
 - [5] R. Panajotovic, F. Martin, P. Cloutier, and L. Sanche, *Radiat. Res.* **165**, 452 (2006).

- [6] For a recent review, see L. Sanche, *Eur. Phys. J. D* **35**, 367 (2005).
- [7] M. A. Huels, I. Hahndorf, E. Illenberger, and L. Sanche, *J. Chem. Phys.* **108**, 1309 (1998).
- [8] H. Abdoul-Carime, M. A. Huels, E. Illenberger, and L. Sanche, *J. Am. Chem. Soc.* **123**, 5354 (2001).
- [9] M.-A. Hervé du Penhoat, M. A. Huels, P. Cloutier, J.-P. Jay-Gerin, and L. Sanche, *J. Chem. Phys.* **114**, 5755 (2001).
- [10] H. Abdoul-Carime, P. Cloutier, and L. Sanche, *Radiat. Res.* **155**, 625 (2001).
- [11] R. Abouaf, J. Pommier, and H. Dunet, *Int. J. Mass Spectrom.* **226**, 397 (2003).
- [12] S. Denifl, S. Ptasińska, M. Cingel, S. Matejcik, P. Scheier, and T. D. Märk, *Chem. Phys. Lett.* **377**, 74 (2003).
- [13] S. Gohlke, H. Abdoul-Carime, and E. Illenberger, *Chem. Phys. Lett.* **380**, 595 (2003).
- [14] G. Hanel B. Gstir, S. Denifl, P. Scheier, M. Probst, B. Farizon, M. Farizon, E. Illenberger, and T. D. Märk, *Phys. Rev. Lett.* **90**, 188104 (2003).
- [15] A. M. Scheer, K. Aflatooni, G. A. Gallup, and P. D. Burrow, *Phys. Rev. Lett.* **92**, 068102 (2004).
- [16] H. Abdoul-Carime, S. Gohlke, and E. Illenberger, *Phys. Rev. Lett.* **92**, 168103 (2004).
- [17] S. Denifl, S. Ptasińska, M. Probst, J. Hrušak, P. Scheier, and T. D. Märk, *J. Phys. Chem. A* **108**, 6562 (2004).
- [18] S. Denifl, S. Ptasińska, G. Hanel, B. Gstir, M. Probst, P. Scheier, and T. D. Märk, *J. Chem. Phys.* **120**, 6557 (2004).
- [19] S. Feil, K. Gluch, S. Matt-Leubner, P. Scheier, J. Limtrakul, M. Probst, H. Deutsch, K. Becker, A. Stamatovic, and T. D. Märk, *J. Phys. B* **37**, 3013 (2004).
- [20] H. Abdoul-Carime, J. Langer, M. A. Huels, and E. Illenberger, *Eur. Phys. J. D* **35**, 399 (2005).
- [21] R. Abouaf and H. Dunet, *Eur. Phys. J. D* **35**, 405 (2005).
- [22] K. Aflatooni, A. M. Scheer, and P. D. Burrow, *Chem. Phys. Lett.* **408**, 426 (2005).
- [23] A. M. Scheer, C. Silvernail, J. A. Belot, K. Aflatooni, G. A. Gallup, and P. D. Burrow, *Chem. Phys. Lett.* **411**, 46 (2005).
- [24] S. Ptasińska, S. Denifl, V. Grill, T. D. Märk, P. Scheier, S. Gohlke, M. A. Huels, and E. Illenberger, *Angew. Chem. Int. Ed.* **44**, 1647 (2005).
- [25] S. Ptasińska, S. Denifl, B. Mróz, M. Probst, V. Grill, E. Illenberger, P. Scheier, and T. D. Märk, *J. Chem. Phys.* **123**, 124302 (2005).

- [26] S. Ptasinska, S. Denifl, P. Scheier, E. Illenberger, and T. D. Märk, *Angew. Chem. Int. Ed.* **44**, 6941 (2005).
- [27] P. D. Burrow, G. A. Gallup, A. M. Scheer, S. Denifl, S. Ptasinska, T. Märk, and P. Scheier, *J. Chem. Phys.* **124**, 124310 (2006).
- [28] S. Denifl, F. Zappa, I. Mähr, J. Lecointre, M. Probst, T. D. Märk, and P. Scheier, *Phys. Rev. Lett.* **97**, 043201 (2006).
- [29] K. Aflatooni, A. M. Scheer, and P. D. Burrow, *J. Chem. Phys.* **125**, 054301 (2006).
- [30] D. Huber, M. Beikircher, S. Denifl, F. Zappa, S. Matejcik, A. Bacher, V. Grill, T. D. Märk, and P. Scheier, *J. Chem. Phys.* **125**, 084304 (2006).
- [31] I. I. Shafranyosh, M. I. Sukhoviya, and M. I. Shafranyosh, *J. Phys. B* **39**, 4155 (2006).
- [32] M. Isaacson, *J. Chem. Phys.* **56**, 1803 (1972).
- [33] M. A. Dillon, H. Tanaka, and D. Spence, *Radiat. Res.* **117**, 1 (1989).
- [34] R. Abouaf, J. Pommier, and H. Dunet, *Chem. Phys. Lett.* **381**, 486 (2003).
- [35] P. L. Levesque, M. Michaud, and L. Sanche, *Nucl. Inst. Meth. B* **208**, 225 (2003).
- [36] R. Abouaf, J. Pommier, H. Dunet, P. Quan, P.-C. Nam, and M. T. Nguyen, *J. Chem. Phys.* **121**, 11668 (2004).
- [37] P. L. Levesque, M. Michaud, W. Cho, and L. Sanche, *J. Chem. Phys.* **122**, 224704 (2005).
- [38] S. Denifl, S. Ptasinska, B. Gstir, P. Scheier, and T. D. Märk, *Int. J. Mass Spectrom.* **232**, 99 (2004).
- [39] K. Aflatooni, G. A. Gallup, and P. D. Burrow, *J. Phys. Chem. A* **102**, 6205 (1998).
- [40] P. Mozejko and L. Sanche, *Radiat. Environ. Biophys.* **42**, 201 (2003).
- [41] F. A. Gianturco and R. R. Lucchese, *J. Chem. Phys.* **120**, 7446 (2004).
- [42] A. Grandi, F. A. Gianturco, and N. Sanna, *Phys. Rev. Lett.* **93**, 048103 (2004).
- [43] S. Tonzani and C. H. Greene, *J. Chem. Phys.* **124**, 054312 (2006).
- [44] P. D. Burrow, *J. Chem. Phys.* **122**, 087105 (2005).
- [45] C. Winstead and V. McKoy, *J. Chem. Phys.* **125**, 174304 (2006).
- [46] R. Barrios, P. Skurski, and J. Simons, *J. Chem. Phys.* **106**, 7991 (2002).
- [47] J. Berdys, I. Anusiewicz, P. Skurski, and J. Simons, *J. Phys. Chem. A* **108**, 2999 (2004).
- [48] J. Berdys, P. Skurski, and J. Simons, *J. Phys. Chem. B* **108**, 5800 (2004).
- [49] I. Anusiewicz, J. Berdys, M. Sobczyk, P. Skurski, and J. Simons, *J. Phys. Chem A* **108**, 11381 (2004).

- [50] X. Li, M. D. Sevilla, and L. Sanche, *J. Am. Chem. Soc.* **125**, 13668 (2003).
- [51] X. Li, L. Sanche, and M. D. Sevilla, *Radiat. Res.* **165**, 721 (2006).
- [52] N. A. Richardson, J. Gu, S. Wang, Y. Xie, and H. F. Schaefer III, *J. Am. Chem. Soc.* **126**, 4404 (2004).
- [53] J. Gu, Y. Xie, and H. F. Schaefer III, *J. Am. Chem. Soc.* **127**, 1053 (2005).
- [54] J. Gu, Y. Xie, and H. F. Schaefer III, *J. Phys. Chem. B* **109**, 13067 (2005).
- [55] R. Hou, J. Gu, Y. Xie, X. Yi, and H. F. Schaefer III, *J. Phys. Chem. B* **109**, 22053 (2005).
- [56] J. Gu, Y. Xie, and H. F. Schaefer III, *J. Am. Chem. Soc.* **128**, 1250 (2006).
- [57] X. Bao, J. Wang, J. Gu, and J. Leszczynski, *Proc. Natl. Acad. Sci. U. S.* **103**, 5658 (2006).
- [58] J. Gu, J. Wang, and J. Leszczynski, *J. Am. Chem. Soc.* **128**, 9322 (2006).
- [59] J. Gu, Y. Xie, and H. F. Schaefer III, *J. Phys. Chem. B* **110**, 19696 (2006).
- [60] Y. Zheng, P. Cloutier, D. J. Hunting, J. R. Wagner, and L. Sanche, *J. Am. Chem. Soc.* **126**, 1002 (2004).
- [61] Y. Zheng, P. Cloutier, D. J. Hunting, L. Sanche, and J. R. Wagner, *J. Am. Chem. Soc.* **127**, 16592 (2005).
- [62] Y. Zheng, P. Cloutier, D. J. Hunting, J. R. Wagner, and L. Sanche, *J. Chem. Phys.* **124**, 064710 (2006).
- [63] C. König, J. Kopyra, I. Bald, and E. Illenberger, *Phys. Rev. Lett.* **97**, 018105 (2006).
- [64] S. Ptasińska, S. Denifl, P. Scheier, and T. D. Märk, *J. Chem. Phys.* **120**, 8505 (2004).
- [65] P. Mozejko and L. Sanche, *Radiat. Phys. Chem.* **73**, 77 (2005).
- [66] X. Pan and L. Sanche, *Chem. Phys. Lett.* **421**, 404 (2006).
- [67] I. Bald, J. Kopyra, and E. Illenberger, *Angew. Chem. Int. Ed.* **45**, 4851 (2006).
- [68] C. Winstead and V. McKoy, *J. Chem. Phys.* **125**, 074302 (2006).
- [69] S. Tonzani and C. H. Greene, *J. Chem. Phys.* **125**, 094504 (2006).
- [70] M. Lepage, S. Letarte, M. Michaud, F. Motte-Tollet, M.-J. Hubin-Franskin, D. Roy, and L. Sanche, *J. Chem. Phys.* **109**, 5980 (1998).
- [71] D. Antic, L. Parenteau, M. Lepage, and L. Sanche, *J. Phys. Chem. B* **103**, 6611 (1999).
- [72] D. Antic, L. Parenteau, and L. Sanche, *J. Phys. Chem. B* **104**, 4711 (2000).
- [73] S.-P. Breton, M. Michaud, C. Jäggle, P. Swiderek, and L. Sanche, *J. Chem. Phys.* **121**, 11240 (2004).
- [74] A. Zecca, C. Perazzolli, and M. J. Brunger, *J. Phys. B* **38**, 2079 (2005).

- [75] A. R. Milosavljević, A. Giuliani, D. Šević, M.-J. Hubin-Franskin, and B. P. Marinković, *Eur. Phys. J. D* **35**, 411 (2005).
- [76] D. Bouchiha, J. D. Gorfinkiel, L. G. Caron, and L. Sanche, *J. Phys. B* **39**, 975 (2006).
- [77] C. N. Trevisan, A. E. Orel, and T. N. Rescigno, *J. Phys. B* **39**, L255 (2006).
- [78] P. Mozejko, E. Ptasińska-Denga, A. Domaracka, and Cz. Szmytkowski, *Phys. Rev. A* **74**, 012708 (2006).
- [79] P. Sulzer, S. Ptasinska, F. Zappa, B. Mielewska, A. R. Milosavljevic, P. Scheier, T. D. Märk, I. Bald, S. Gohlke, M. A. Huels, and E. Illenberger, *J. Chem. Phys.* **125**, 044304 (2006).
- [80] A. R. Milosavljević, F. Blanco, D. Šević, G. García, and B. P. Marinković, *Eur. Phys. J. D* **40**, 107 (2006).
- [81] P. Mozejko, A. Domaracka, E. Ptasińska-Denga, and Cz. Szmytkowski, *Chem. Phys. Lett.* **429**, 378 (2006).
- [82] H. Abdoul-Carime, S. Gohlke, E. Fischbach, J. Scheike, and E. Illenberger, *Chem. Phys. Lett.* **387**, 267 (2004).
- [83] S. Deniff, P. Candori, S. Ptasińska, P. Limão-Vieira, V. Grill, T. D. Märk, and P. Scheier, *Eur. Phys. J. D* **35**, 391 (2005).
- [84] K. Takatsuka and V. McKoy, *Phys. Rev. A* **24**, 2473 (1981).
- [85] K. Takatsuka and V. McKoy, *Phys. Rev. A* **30**, 1734 (1984).
- [86] C. Winstead and V. McKoy, *Adv. At. Mol. Opt. Phys.* **36**, 183 (1996).
- [87] C. Winstead and V. McKoy, *Comput. Phys. Commun.* **128**, 386 (2000).
- [88] M. W. Schmidt, K. K. Baldrige, J. A. Boatz, S. T. Elbert, M. S. Gordon, J. H. Jensen, S. Koseki, N. Matsunaga, K. A. Nguyen, S. J. Su, T. L. Windus, M. Dupuis, and J. A. Montgomery, *J. Comput. Chem.* **14**, 1347 (1993).
- [89] M. J. Frisch, G. W. Trucks, H. B. Schlegel, P. M. W. Gill, B. G. Johnson, M. A. Robb, J. R. Cheeseman, T. Keith, G. A. Petersson, J. A. Montgomery, K. Raghavachari, M. A. Al-Laham, V. G. Zakrzewski, J. V. Ortiz, J. B. Foresman, J. Cioslowski, B. B. Stefanov, A. Nanayakkara, M. Challacombe, C. Y. Peng, P. Y. Ayala, W. Chen, M. W. Wong, J. L. Andres, E. S. Replogle, R. Gomperts, R. L. Martin, D. J. Fox, J. S. Binkley, D. J. Defrees, J. Baker, J. P. Stewart, M. Head-Gordon, C. Gonzalez, and J. A. Pople, *Gaussian 94, Revision D.4*, (Gaussian, Inc., Pittsburgh PA, 1995).
- [90] N. Foloppe and A. D. MacKerell, Jr., *Biophys. J.* **76**, 3206 (1999).

- [91] G.Schaftenaar and J.H. Noordik, *J. Comput.-Aided Mol. Design* **14**, 123 (2000).
- [92] T.H. Dunning, Jr., and P. J. Hay, in *Methods of Electronic Structure Theory*, H. F. Schaefer III, ed. (Plenum, New York, 1977), p. 1.
- [93] T.H. Dunning, Jr., *J.Chem.Phys.* **55**, 716 (1971).
- [94] C. W. Bauschlicher, *J. Chem. Phys.* **72**, 880 (1980).
- [95] V. I. Lebedev and D. N. Laikov, *Dokl. Akad. Nauk* **366**, 741 (1999) [*Dokl. Math.* **59**, 477 (1999)], and references therein.
- [96] T. N. Rescigno and B. I. Schneider, *Phys. Rev. A* **45**, 2894 (1992), and references therein.
- [97] S. Tonzani and C. H. Greene, *J. Chem. Phys.* **122**, 014111 (2005).
- [98] W. Chin, M. Mons, I. Dimicoli, F. Piuzzi, B. Tardivel, and M. Elhaine, *Eur. Phys. J. D* **20**, 347 (2002), and references therein.
- [99] Chr. Plützer, E. Nir, M. S. de Vries, and K. Kleinermanns, *Phys. Chem. Chem. Phys.* **3**, 5466 (2001).

V. FIGURE CAPTIONS

FIGURE 1. (Color online) The molecules considered in the present work. On the top row are the purine bases guanine (left) and adenine (right); on the bottom row, left to right, are the nucleosides 2'-deoxyguanosine and 2'-deoxyadenosine and the nucleotide 2'-deoxyadenosine 5'-monophosphate. Oxygen is red (dark), carbon brown (medium), nitrogen blue (light), and hydrogen white; phosphorous is the light-yellow sphere surrounded by four oxygens.

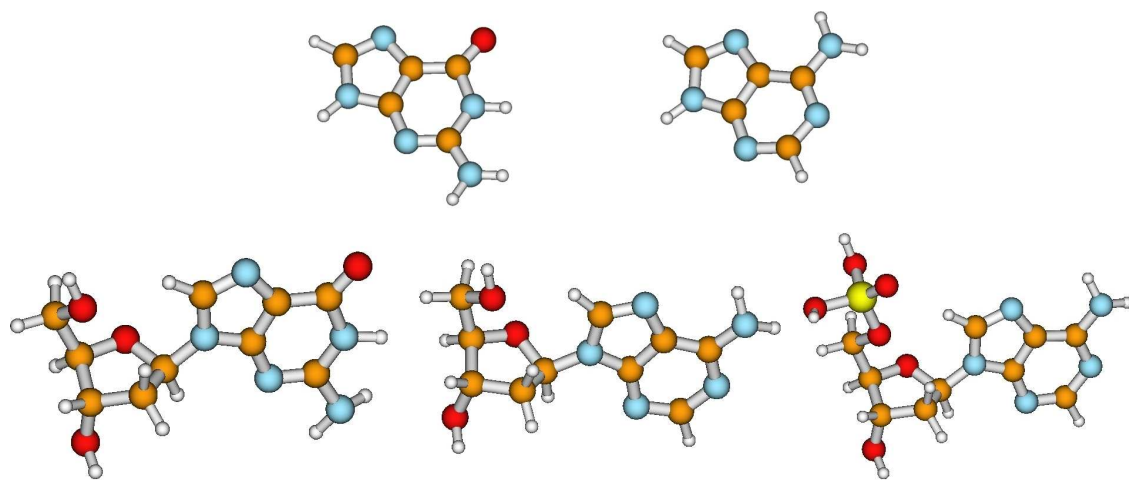
FIGURE 2. (Color online) Integral elastic cross sections for adenine computed in the static-exchange approximation using different basis sets: Basis I (chained, violet), Basis II (red, dashed), Basis III (green, dotted), and Basis IV (blue, solid). The top panel shows results for the A' component of the C_s point group and the bottom panel for the A'' component, where the π^* resonances occur.

FIGURE 3. (Color online) A'' component of the low-energy integral cross section for elastic scattering of electrons by adenine computed in the SEP approximation.

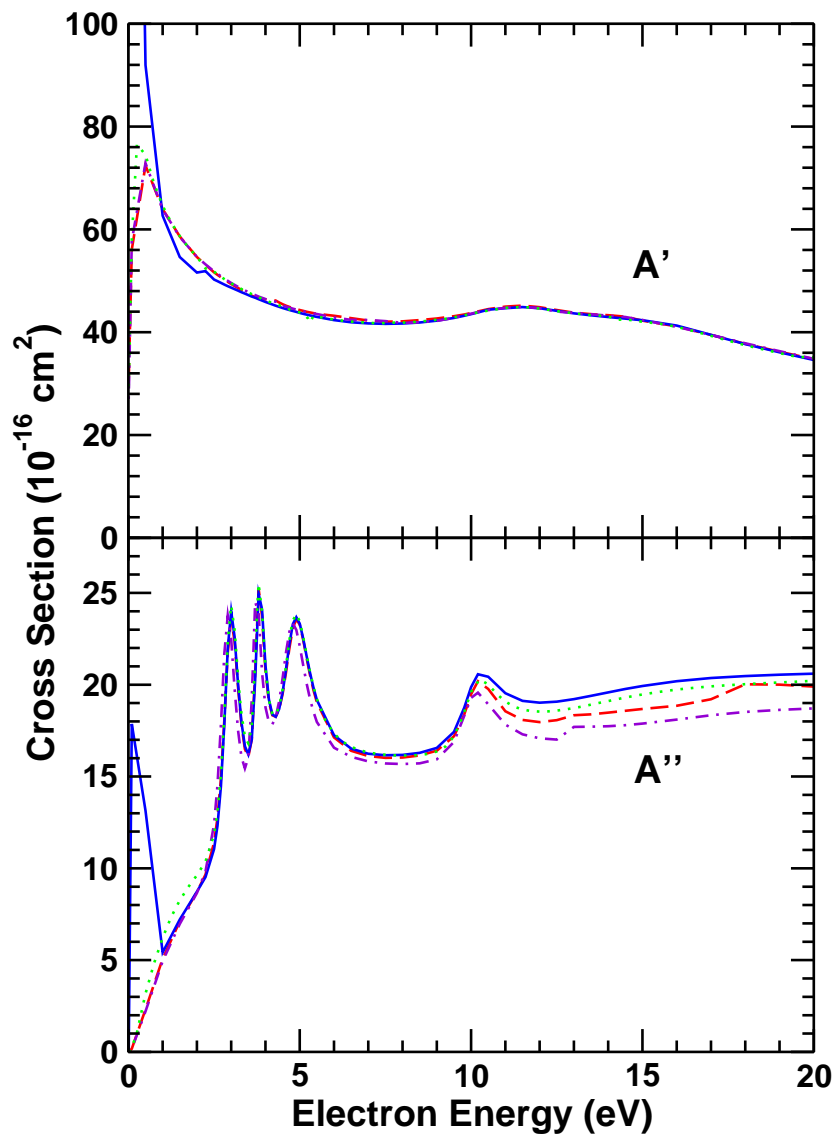
FIGURE 4. (Color online) Integral elastic cross sections for guanine computed in the static-exchange approximation using basis set Basis III. Components of the cross section obtained in C_s symmetry are shown in the top two panels. The bottom panel compares the summed C_s cross section (dotted blue line) with the integral cross section obtained using the fully-optimized C_1 nuclear geometry (solid red line).

FIGURE 5. (Color online) A'' component of the low-energy integral cross section for elastic scattering of electrons by guanine computed in the SEP approximation.

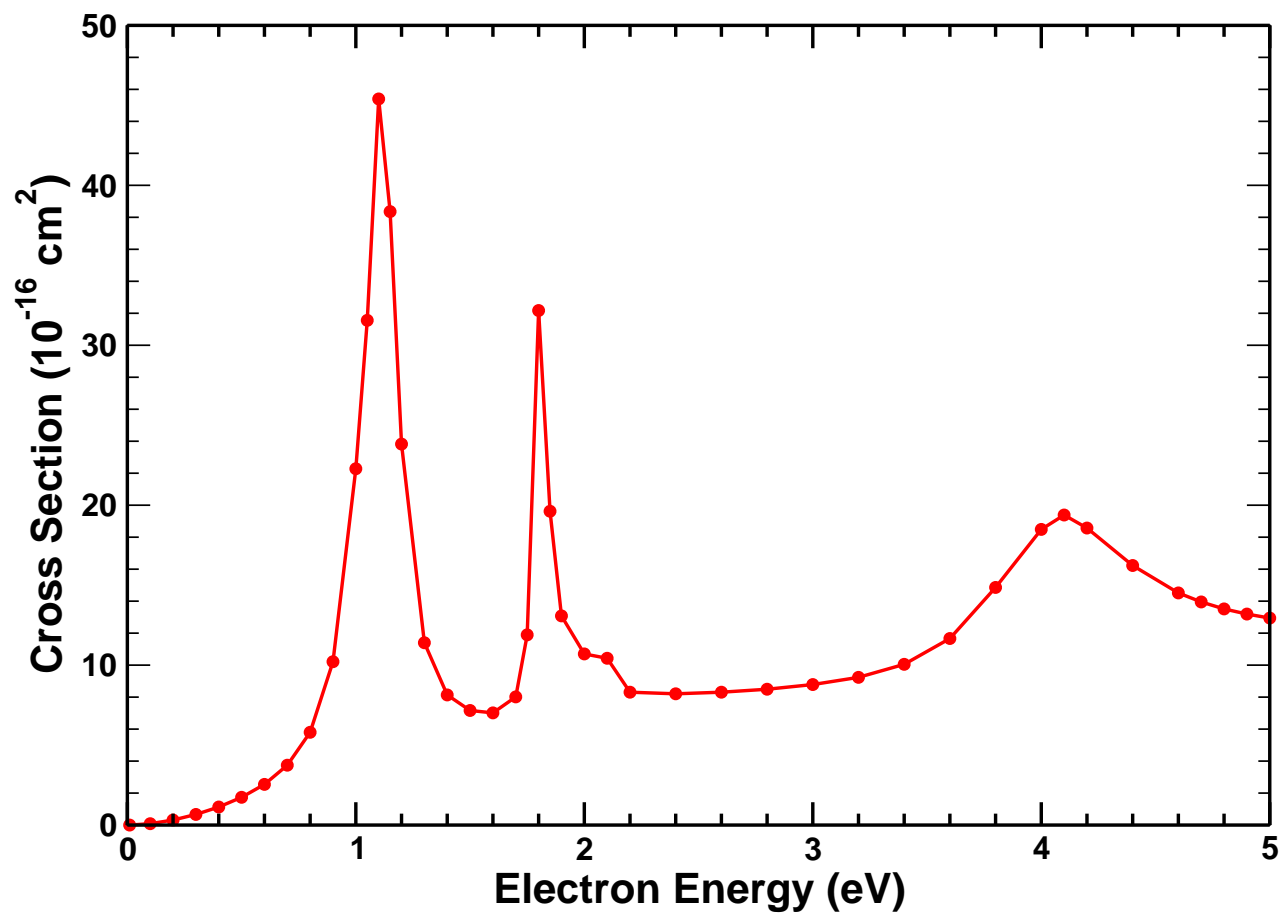
FIGURE 6. (Color online) Integral elastic electron scattering cross sections for the nucleosides 2'-deoxyguanosine (dashed red line), 2'-deoxyadenosine (chained green line), and the nucleotide 2'-deoxyadenosine 5'-monophosphate (solid blue line), computed in the static-exchange approximation.



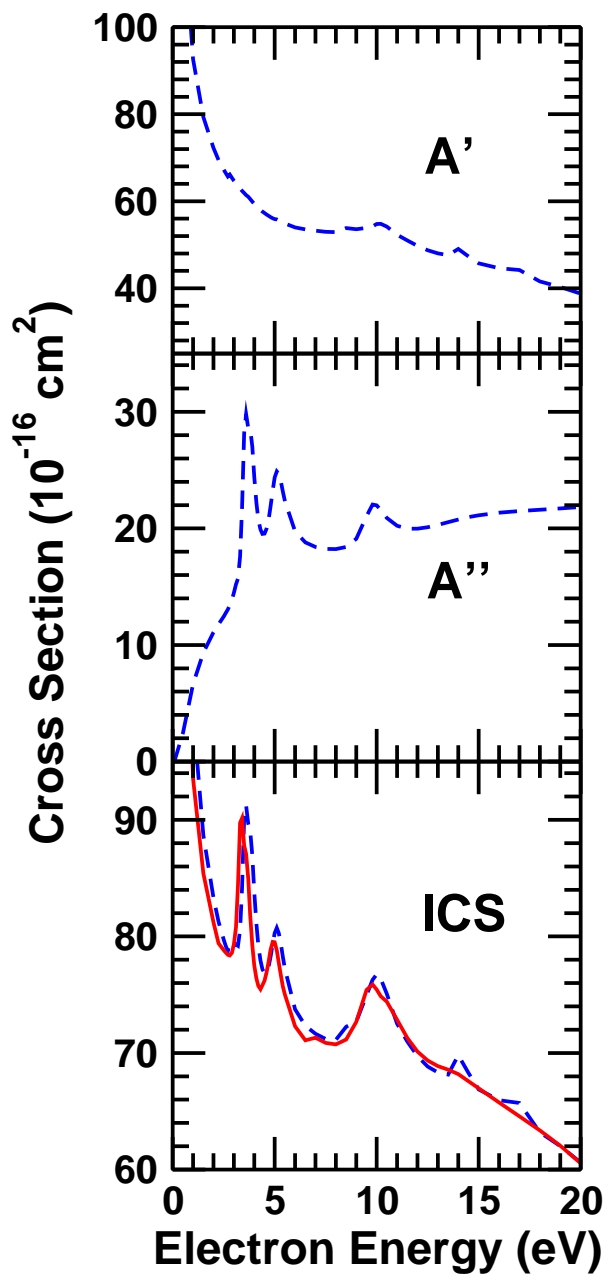
Winstead and McKoy, Fig. 1



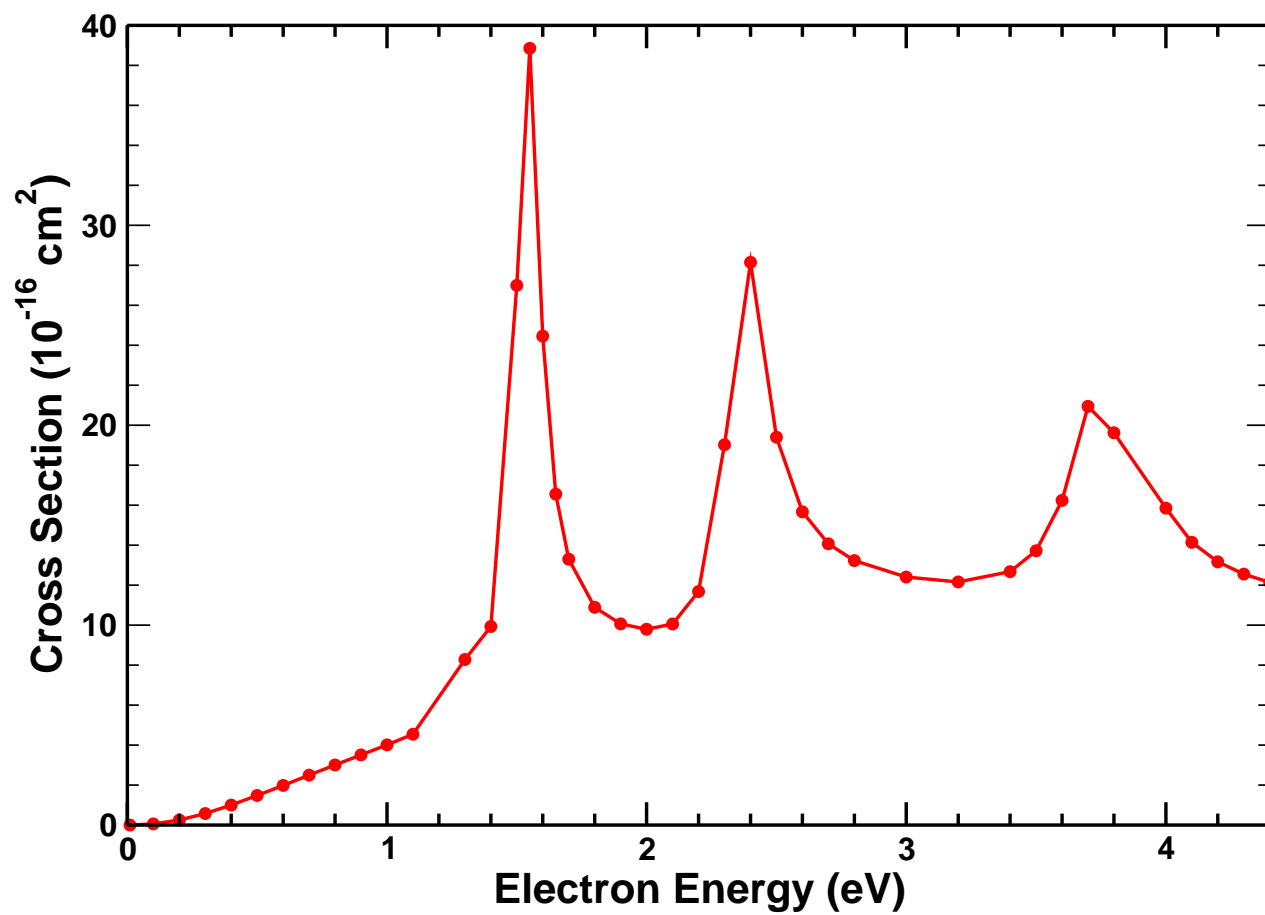
Winstead and McKoy, Fig. 2



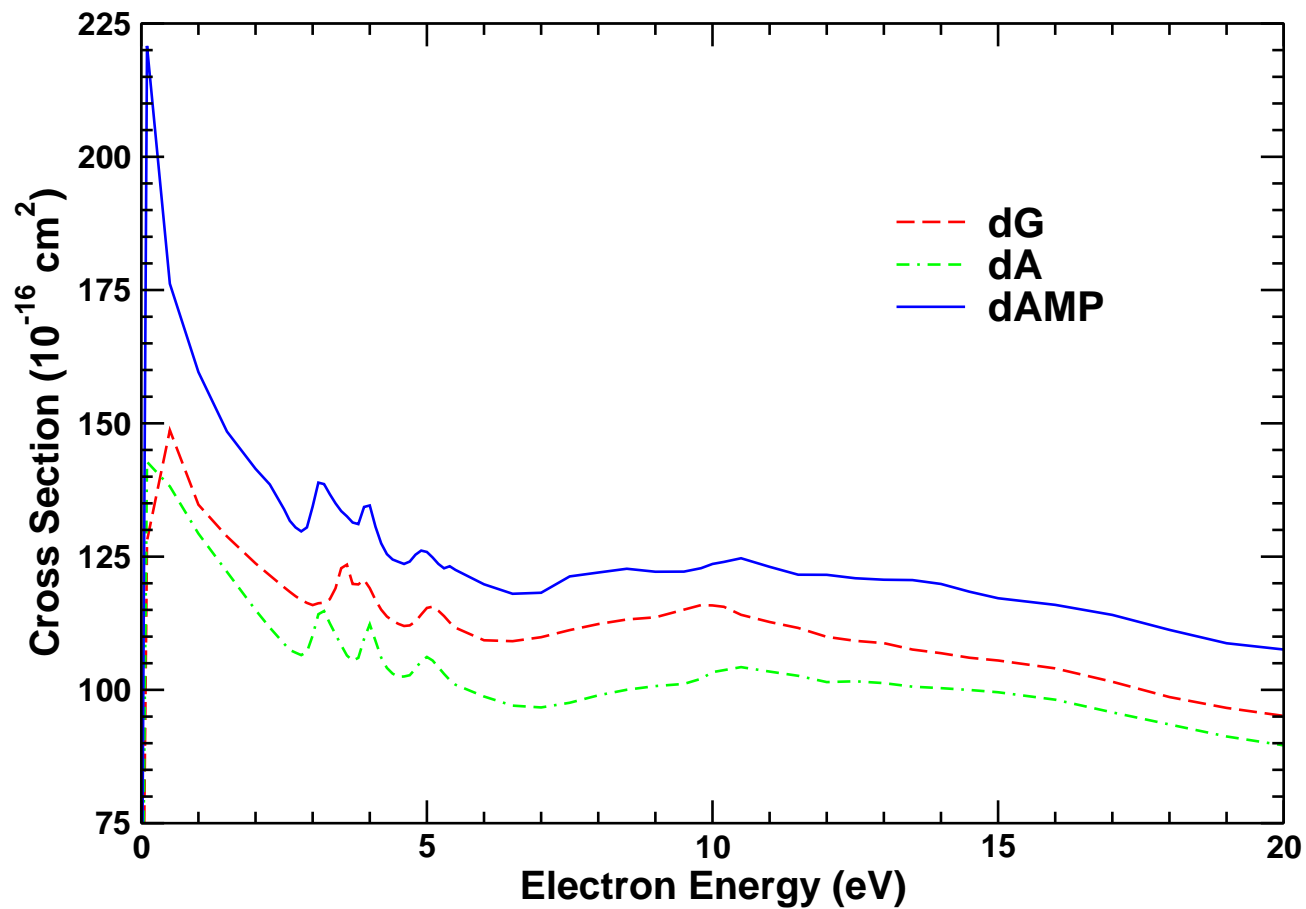
Winstead and McKoy, Fig. 3



Winstead and McKoy, Fig. 4



Winstead and McKoy, Fig. 5



Winstead and McKoy, Fig. 6